A method to identify physical, chemical and biological factors that trigger Bcl-xL-mediated apoptosis

Aleksandr Ianevski [1], Evgeny Kulesskiy [2], Klara Krpina [1], Guofeng Lou [3], Yahyah Aman [3], Andrii Bugai [4], Koit Aasumets [5], Yevhen Akimov [2], Daria Bulanova [2], Kiira Gildemann [5], Albert F. Arutyunyan [6], Olga Yu. Susova [7], Alexei L. Zhuze [6], Valentyn Oksenych [1], Hilde Lysvand [1], Joachim M. Gerhold [5], Magnar Bjørås [1], Pål Johansen [8], Anders Waage [1], Caroline Heckman [2], Evandro F. Fang [3], Denis E. Kainov [1,2,5] *

[1] Department of Clinical and Molecular Medicine, Norwegian University of Science and Technology, Trondheim 7028, Norway.

[2] Institute for Molecular Medicine Finland, FIMM, University of Helsinki 00014, Finland

[3] Department of Clinical Molecular Biology, University of Oslo and Akershus University Hospital, Lørenskog 1478, Norway

[4] Department of Biochemistry and Developmental Biology, University of Helsinki, Helsinki 00014, Finland

[5] Institute of Technology, University of Tartu, Tartu 50090, Estonia

[6] Engelhardt Institute of Molecular Biology Russian Academy of Sciences, Moscow 119991, Russia

[7] Institute of Carcinogenesis, FSBI "N.N. Blokhin National Medical Research Center of Oncology", The Ministry of Health of the Russian Federation, Moscow, Russia

[8] Department of Dermatology, University of Zurich, Zurich, Switzerland

* To whom correspondence should be addressed. Tel: +358405490220; Fax: +358405490220; Email: denis.kainov@ntnu.no

ABSTRACT

We demonstrated recently that different viruses and transfected viral RNA or plasmid DNA killed human non-malignant cells sensitized with Bcl-xL-specific inhibitor A-1155463. Here, we show that DNA-damaging agent 4-nitroquinoline-1-oxide (4NQO) killed human non-malignant as well as malignant cells and the small roundworm C. elegans when combined with A-1155463, but not with Bcl-2- or Mcl-1-specific agents. The synergistic effect of 4NQO-A-1155463 combination was p53 dependent and was associated with the release of Bad and Bax from Bcl-xL, indicating that Bcl-xL linked DNA damage response pathways, p53 signalling and apoptosis. Other anticancer drugs (i.e. amsacrine, SN38, cisplatin, mitoxantrone, dactinomycin. dinaciclib, UCN-01, bortezomib, and S63845), as well as birth-control drug 17α-ethynylestradiol, immunosuppressant cyclosporin, antiviral agent brincidofovir, DNA binding probes MB2Py(Ac), DB2Py(4) and DBPy(5) and UV radiation also killed A-1155463-sensitized non-malignant cells. Thus, we established a method to identify physical, chemical and biological factors, which trigger Bcl-xL-mediated apoptosis. The method could be used in the development of novel anticancer therapies based on systemic Bcl-xL-specific inhibitor and local radiation, oncolytic virus infection or chemotherapy.

INTRODUCTION

Apoptosis is a tightly regulated process that kills cells with severely damaged or invasive DNA, RNA, and proteins (Elmore, 2007, Shim, Kim et al., 2017). When apoptosis is inhibited, cells that should be eliminated may persist and become malignant (Wong, 2011).

B-cell lymphoma 2 (Bcl-2) family of proteins are key players in apoptosis (Kale, Osterlund et al., 2018). For example, Bcl-xL, Bcl-2 and Mcl-1 are anti-apoptotic, whereas Bax, Bak and Bad are pro-apoptotic members of the family (Denisova, Kakkola et al., 2012, Fernandez, Sebti et al., 2018, Kuivanen, Bespalov et al., 2017). Interaction between pro- and anti-apoptotic proteins determine the fate of a cell. In particular, alteration of the interactions could lead to release of Bax and Bak which could form a pore in the mitochondrial outer membrane that allowed cytochrome C to escape into the cytoplasm and activate the caspase cascade (Shamas-Din, Kale et al., 2013).

Several chemical inhibitors were developed to bind anti-apoptotic of Bcl-2 proteins and induce cancer cells death (Adams, Clark-Garvey et al., 2018). These small molecules belong to several structurally distinct classes (Fig. S1a). First class of Bcl2i includes ABT-737 and its derivatives ABT-263 (navitoclax) and ABT-199 (venetoclax); second class includes WEHI-539 and its derivatives, A-1331852 and A-1155463. There are other classes of Bcl-2 inhibitors containing structurally similar molecules, such as S63845 and S64315, S55746 and A1210477.

The inhibitors have different affinities to Bcl-2 protein family members (Fig. S1b). For example, ABT-199 has a high affinity to Bcl-2; WEHI-539, A-1331852 and A-1155463 are specific for Bcl-xL; S63845, S64315, S55746 and A1210477 have high affinity to Mcl-1; whereas ABT-263 binds Bcl-2, Bcl-xL and Bcl-w with similar affinity. Importantly, ABT-199 was approved, whereas ABT-263, S63845 and several other Bcl-2 inhibitors are currently in clinical trials against blood cancers and solid tumours (Casara, Davidson et al., 2018, King, Peterson et al., 2017, Korycka-Wolowiec, Wolowiec et al., 2019, Timucin, Basaga et al., 2019) (NCT02920697). These drugs provide opportunities for treatment of hematologic and other types of cancers, but also create new challenges associated with emerging drug resistance of cancer cells and toxicity for non-cancer cells (e.g. thrombocytopaenia).

To obtain additive or synergistic effects, enhance efficacy of treatment and combat genetically heterogeneous cancers, Bcl-2 inhibitors were combined with other anticancer drugs (Fig. S1c; bcl2icombi.info) (Chen, Jin et al., 2011, Haikala, Anttila et al., 2019, Jeong, Oh et al., 2019, Shen, Li et al., 2018). The drug combinations were also used to lower the dose of Bcl-2 inhibitors to overcome resistance and toxicity issues for non-malignant cells (Adams et al., 2018). Dozens of the drug combinations have been reported to be active *in vitro* (cell culture, patient-derived cells or organoids) and *in vivo* (patient-derived xenograft mouse models). In addition, 109 combinations (excluding combinations with biological agents) were in clinical trials. However, only ABT-199 in combination with azacytidine, decitabine or cytarabine was approved for the treatment of acute myeloid leukaemia (AML).

Clinical trials with 31 combinations have been terminated, withdrawn or suspended due to adverse effects or other issues. These include trials with ABT-263 plus bendamustine and rituximab in patients with relapsed diffuse large B-cell lymphoma, ABT-263 plus abiraterone acetate with or without

hydroxychloroquine in patients with progressive metastatic castrate refractory prostate cancer, as well as ABT-199 plus RICE (rituximab, ifosfamide, carboplatin, etoposide), or plus rifampin, or plus bortezomib and dexamethasone, ixazomib and carfilzomib (NCT02471391, NCT01423539, NCT03064867, NCT01969682, NCT02755597, NCT03314181, NCT03701321). The identification of the adverse effects prior to clinical trials is challenging but could save lives for many cancer patients.

We noticed that many Bcl-2 inhibitors have been combined with compounds, which damaged cellular DNA, RNA or proteins by targeting DNA replication, RNA transcription and decay, as well as protein signalling and degradation pathways. Here, we shed new light on the mechanisms of actions of such combinations and establish a method for identification of chemical, physical and biological factors which trigger Bcl-xL-mediated apoptosis.

First, we showed that combination of DNA-damaging agent 4-nitroquinoline-1-oxide (4NQO) together with Bcl-xL-specific inhibitor A-1155463, but not drugs alone, were toxic for human malignant and non-malignant cells, as well as for C. elegans. The synergistic effect of the drug combination was dependent on p53 expression and associated with the release of Bad and Bax from Bcl-xL. Second, we demonstrated that several anticancer drugs (i.e. amsacrine, SN38, cisplatin, mitoxantrone, dactinomycin. dinaciclib, UCN-01, bortezamib, and S63845), as well as birth-control drug 17α-ethynylestradiol, immunosuppressant cyclosporin, antiviral agent brincidofovir, DNA binding probes MB2Py(Ac), DB2Py(4) and DBPy(5), and UV radiation triggered Bcl-xl-mediated apoptosis in non-malignant cells. Finally, we discussed the application of the method for the development of novel options for treatment of cancer and other diseases.

RESULTS

Toxicity of A-1155463-4NQO combination in C. elegans

We tested DNA-damaging agent 4NQO (Walker & Sridhar, 1975) plus Bcl-xL-specific inhibitor A-1155463 in C. elegans. The worms treated with A-1155463-4NQO combination died faster than those treated with either A-1155463 or 4NQO (Fig. 1a, b). Moreover, the worms treated with the drug combination exhibited defects in reproduction and development (Fig. 1c). The Bliss synergy scores for adult development, L4 development and egg hatching were 19, 21 and 24 respectively. Treatment with A-1155463 or 4NQO alone did not affect these stages. Thus, combination of 4NQO with A-1155463 had a severe impact on the C. elegans lifespan, reproductive system and development.

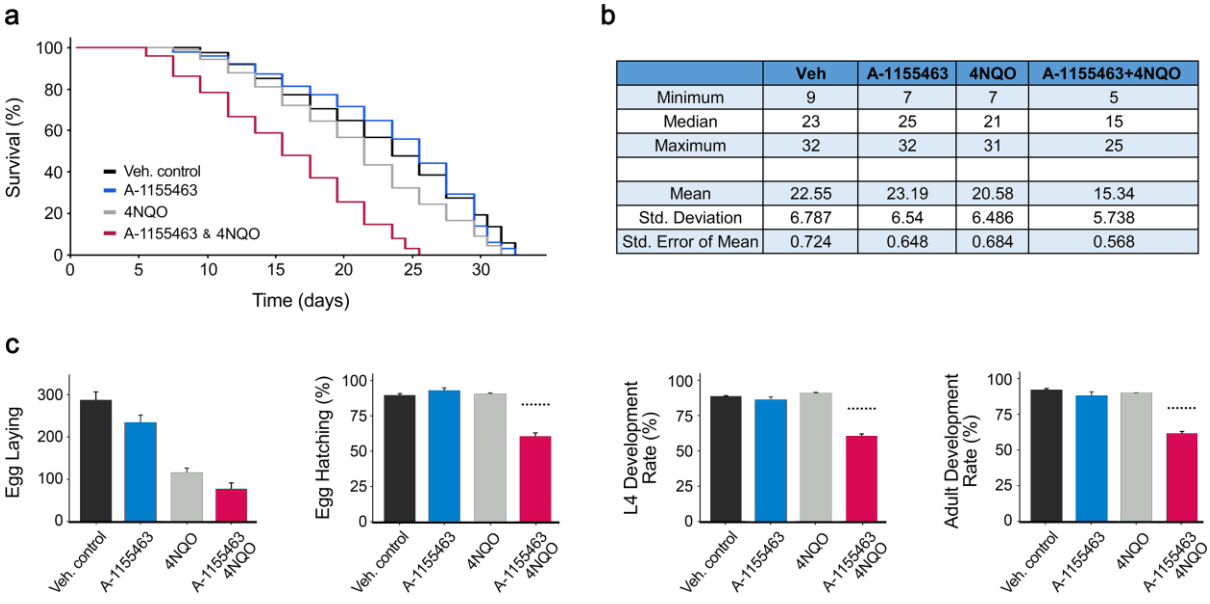

b

	Veh	A-1155463	4NQO	A-1155463+4NQO
Minimum	9	7	7	5
Median	23	25	21	15
Maximum	32	32	31	25
Mean	22.55	23.19	20.58	15.34
Std. Deviation	6.787	6.54	6.486	5.738
Std. Error of Mean	0.724	0.648	0.684	0.568

Figure 1. A combination of Bcl-xL- specific inhibitor A-1155463 and DNA-damaging agent 4NQO exhibits synergistic toxicities on lifespan, reproduction and development to the wild type roundworm C. elegans. (a, b) Kaplan-Meier survival curves of worms challenged with 10 µM A-1155463, 10 µM 4NQO, drug combination or vehicle. The log-rank Mantel–Cox test was used for statistical analysis. (c) Toxicity detection for the different stages of C. elegans reproduction and development after the treatment with 10 µM A-1155463, 10 µM 4NQO or their combination (Mean ± SD). Dotted lines above combination bars represent the expected effect given by Bliss reference model.

Toxicity of A-1155463-4NQO combination for human non-malignant cells

To recapitulate the *in vivo* toxicity of A-1155463-4NQO combination in *in vitro* experiments, we used human non-malignant retinal pigment epithelium (RPE) cells. PRE cells died 3 h after treatment with A-1155463-4NQO combination, whereas majority of cells treated with either A-1155463 or 4NQO remained viable for 24 h as measured by real-time impedance assay (Fig. 2a). Another cell viability assay, which quantified intracellular ATP, demonstrated that the effect of A-1155463-4NQO combination was synergistic (ZIP synergy score, 14±3; Fig. 2b). Similar results were obtained with 4NQO in combination with another Bcl-xL-specific inhibitor, A-133852 (ZIP synergy score, 17±0; Fig. 2c). ABT-263, a pan-Bcl-2 inhibitor, also showed synergy with 4NQO (ZIP synergy score, 8±1; Fig. 2c). In contrast, combinations of 4NQO with the Bcl-2- or Mcl-1-specific inhibitors did not show a synergy (ZIP synergy scores, 3±1 and 2±1, respectively; Fig. 2c). These results suggested that the DNA-damaging agent combined with Bcl-xL-, but not Bcl-2- or Mcl1-specific inhibitors facilitated the death of human non-malignant RPE cells.

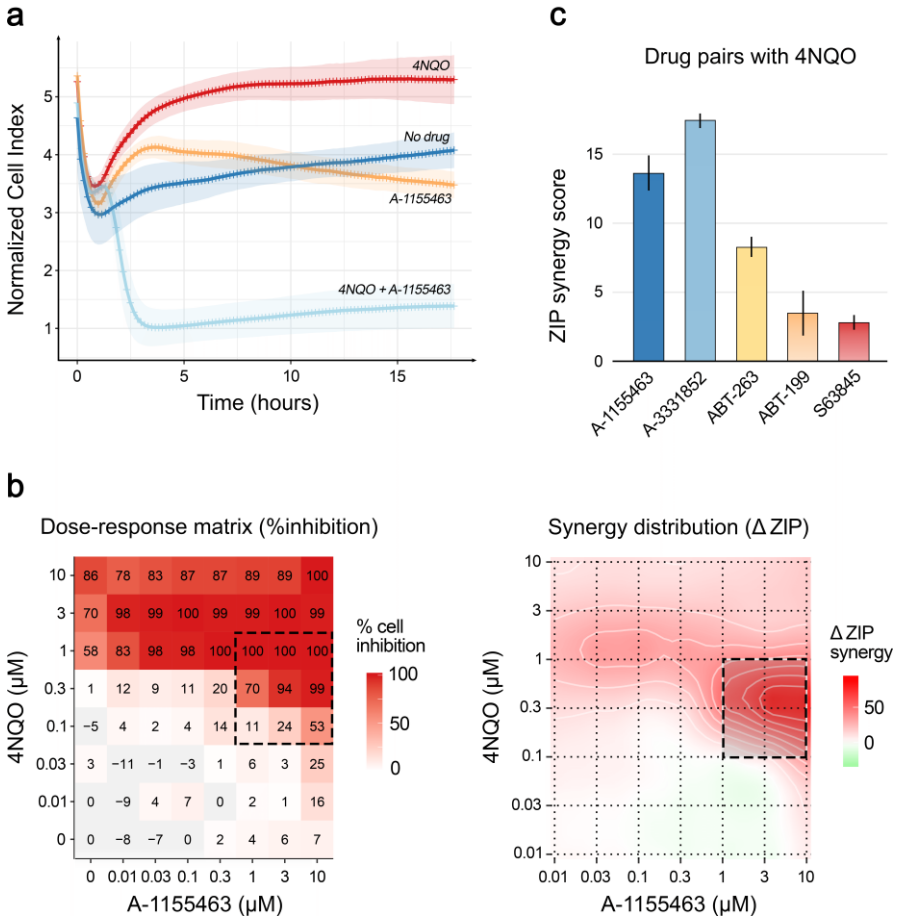

Figure 2. Combinations of DNA-damaging agent 4NQO with Bcl-xL-, but not Bcl-2- or Mcl-1-specific inhibitors, exhibit synergistic toxicities on human non-malignant RPE cells. (a) Real-time impedance traces for RPE cells exposed to 1 μM 4NQO, 1 μM A-1155463 or their combination. Control trace represents cells exposed to 0.1% DMSO (Mean ± SD; n = 8). (b) The interaction landscapes of A-1155463-4NQO drug combination. It represents the net combinational effects on viability of RPE cells, as measured with CTG assays. (c) Synergy scores of combinations of 4NQO and 5 Bcl-2 inhibitors (Mean ± SD; n = 3). RPE cells were treated with different concentrations of Bcl-2 inhibitor and 4NQO. After 24 h cell viability was measured using the CTG assay. Synergy scores were quantified based on the ZIP model.

4NQO induced p53 expression, whereas A-1155463 triggered release of pro-apoptotic Bad and Bax from Bcl-xL in RPE cells

Immunoblot analysis of whole-cell extracts showed that expression of p53, a key regulator of DNA-damage response and Bcl-xL-dependent apoptosis, was induced after 2 h of treatment with 4NQO, but not with A-1155463 in RPE cells (Fig. 3a). Confocal microscopy confirmed this observation. Of note, p53 accumulated in the nucleus of 4NQO-treated cells (Fig. 3b).

Immuno-precipitation of Bcl-xL-interacting partners showed that A-1155463 displaced Bad and Bax from Bcl-xL in RPE cells after 2 h of treatment (Fig. 3a). Confocal microscopy revealed that Bad

dislocated from mitochondria, whereas Bax accumulated in the nucleus of A-1155463-treated cells (Fig. 3c, d).

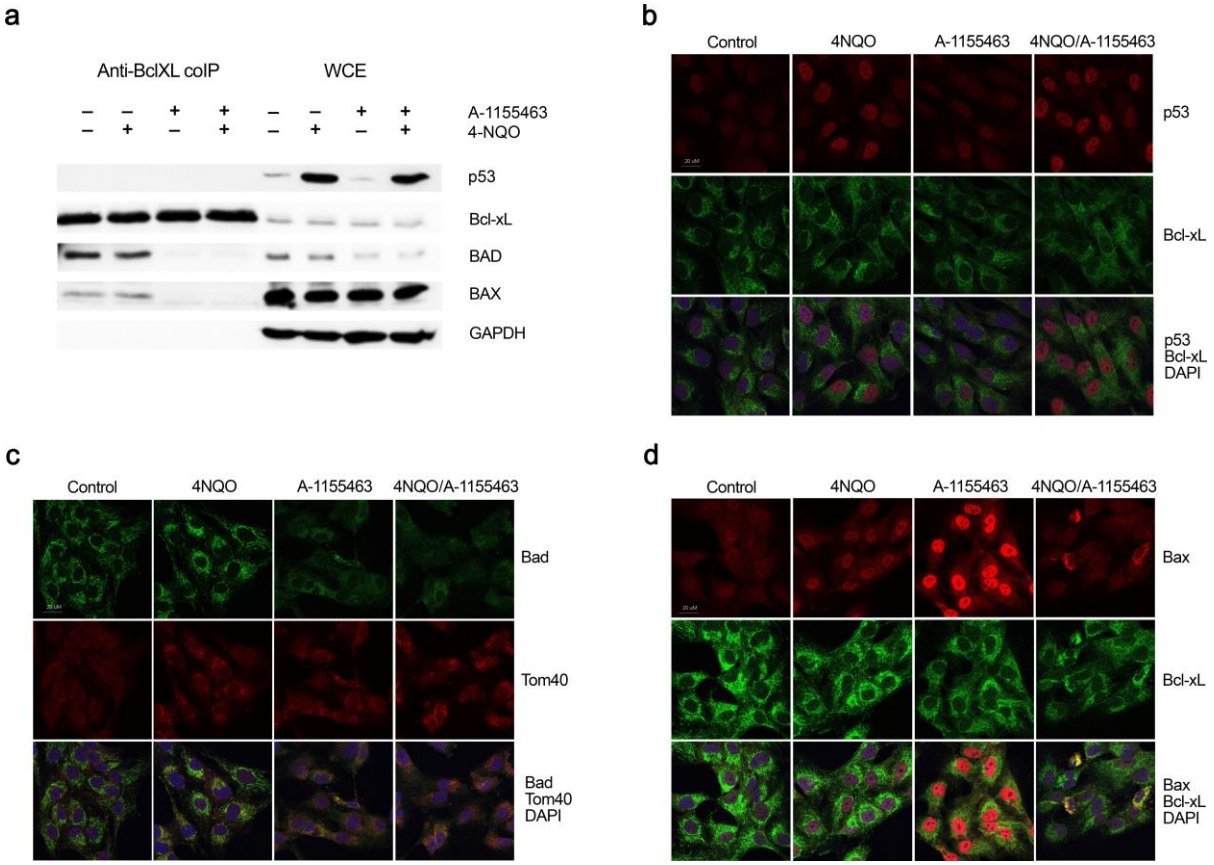

Figure 3. 4NQO mediates induction of p53 expression and A-1155463 triggers release of pro-apoptotic Bad and Bax from Bcl-xL in RPE cells. (a) RPE cells were treated with 1 μM 4NQO, 1 μM A-1155463 or their combination. Control cells were treated with 0.1% DMSO. Whole cell extracts (WCE) were obtained 2 h after treatment. Proteins were immuno-precipitated by anti-Bcl-xL antibody. P53, Bcl-xL, Bad, Bax, and GAPDH were analysed using Western blotting in WCE and immunoprecipitates. (b-d) RPE cells were treated as for (a). Two hours after treatment cells were fixed, and p53, Bcl-xL, Bad, Bax and Tom40 (mitochondria) were stained with corresponding antibodies. Nuclei were stained with DAPI. Cells were imaged using a confocal microscopy. Representative images (n=8) were selected. Scale bar, 20 μm.

The 4NQO-A-1155463 combination induced expression of p53. Moreover, the combination displaced Bad and Bax from Bcl-xL retaining both proteins in the cytoplasm of RPE cells (Fig. 3). Both events could be critical for initiation of apoptosis (Kakkola, Denisova et al., 2013, Lai, Chi et al., 2007). Of note, treatment of RPE cells for 2 h with either 4NQO, or A-1155463 or in combination did not substantially affect general transcription and translation, as well as expression of several apoptotic proteins and phosphorylation of protein kinases (Fig. S2).

p53 is dispensable for A-1155463-4NQO synergy

To confirm the role of p53 in A-1155463-4NQO synergy, we used malignant HCT116 TP53$^{-/-}$ cells, which lacked p53 expression (Fig. 4a). A-1155463-4NQO combination had substantially lower effect on viability, death and early apoptosis of TP53$^{-/-}$ cells (Fig. 4b-d). By contrast, A-1155463-4NQO combination killed malignant HCT116 TP53$^{+/+}$ cells, at the same concentration as RPE cells. These results indicated that p53 was essential for A-1155463-4NQO synergy.

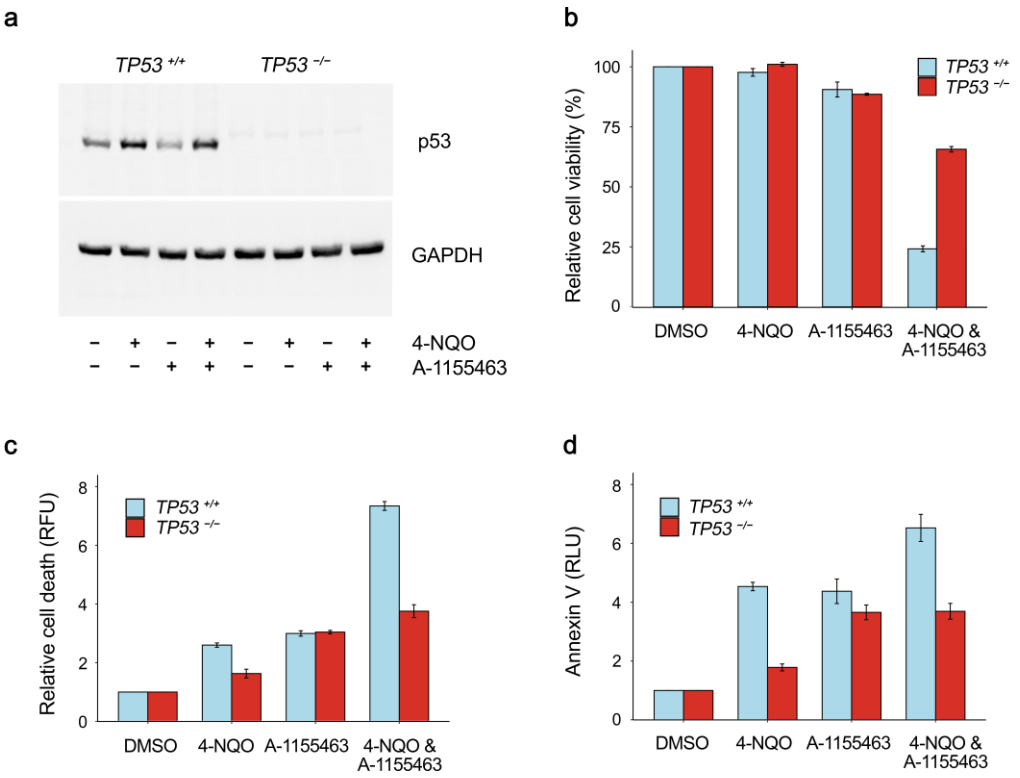

Figure 4. p53 is dispensable for A-1155463-4NQO synergy. (a) HCT116 TP53-/- and TP53+/+ cells were treated with 1 μM 4NQO, 1 μM A-1155463 or their combination. Control cells were treated with 0.1% DMSO. 2 h after treatment p53 and GAPDH were analysed using western blotting of whole-cell extracts. (b) Cells were treated as for (a). Cell viability was measured by the CTG assay. Mean ± SD, n = 3. (c) Cells were treated as for (a). Cell death was measured by the CTxG assay. Mean ± SD, n = 3. (d) Cells were treated as for (a). Apoptosis was measured by the Annexin V assay. Mean ± SD, n = 3.

Synergistic toxicity of different combinations containing Bcl-xL inhibitors and different DNA-, RNA- and protein-damaging agents for RPE cells

We next tested combinations of A-1155463, A-133852, ABT-199, and S63845 with 39 DNA, RNA and protein damaging agents in RPE cells. The experiment revealed that A-133852 and A-1155463 in combination with these agents were highly synergistic, indicating that Bcl-xL was essential for induction of apoptosis in non-malignant cells under chemical insults (Fig. 5a, b). Importantly, hit

compounds induced expression of p53 after 2 h of treatment (Fig. 5c). Interestingly, combinations of S63845 with A-1155463 or A-133852, but not with ABT-199, were highly synergistic and toxic for non-malignant cells indicating that Mcl-1 or another potential cellular target could be damaged by S63845 (Fig. 5d).

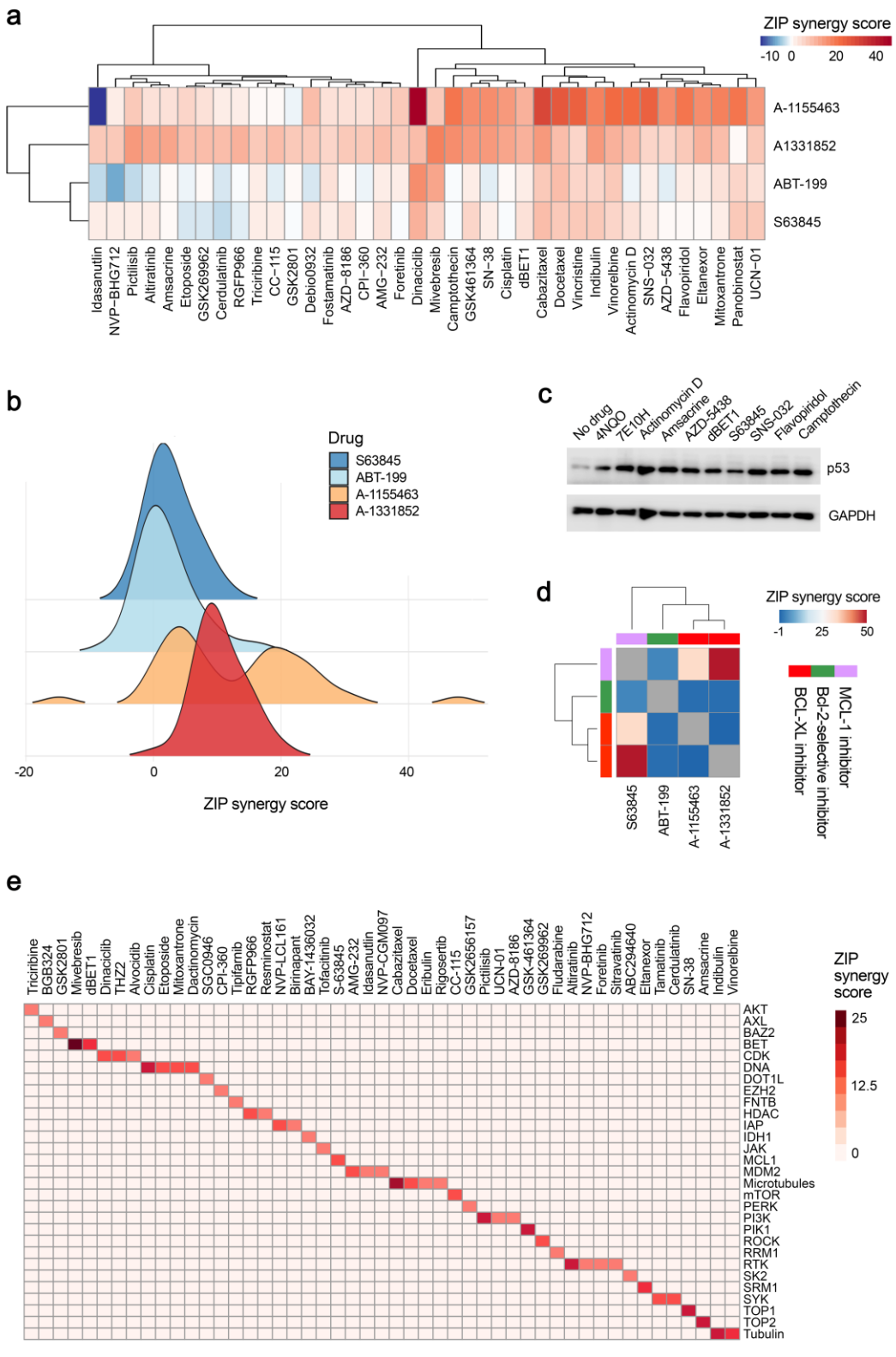

Figure 5. Anticancer agents targeting cellular DNA, RNA, or proteins facilitate death of human non-malignant RPE cells sensitized with Bcl-xL-, but not Bcl-2- or Mcl-1-specific inhibitors. (a) Heatmap showing synergy scores for combinations of four Bcl-2 inhibitors and 39 anticancer agents. RPE cells were treated with 0, 10, 30, 100, 300, 1000, 3000 and 10000 nM Bcl-2 inhibitors and anticancer agents. After 24 h cell viability was measured by the CTG assay. (b) Distribution of synergy scores based on (a). (c) Immunoblot analysis of p53 and GAPDH (loading control) expression levels after 2h of treatment of RPE cells with selected anticancer agents. (d) Heatmap showing synergy scores for combinations of four Bcl-2 inhibitors with each other. RPE cells were treated with 0, 10, 30, 100, 300, 1000, 3000 and 10000 nM Bcl-2 inhibitors and anticancer agents. After 24 h cell viability was measured by the CTG assay. (e) Cellular targets of anticancer agents which showed synergy with A-133852. RPE cells were treated with A-133852 and 527 anticancer agents as for panel (a). After 24 h cell viability was measured using the CTG assay. The compounds with synergy >7.5 were selected and plotted against their targets. ZIP method was used to calculate synergy scores for all panels.

Moreover, screening of A-1331852 with 527 approved and emerging investigational anticancer agents revealed 64 highly synergistic combinations (δ>7.5; Table S2). The hit anticancer agents targeted mainly cellular DNA replication (i.e. amsacrine, SN38, cisplatin, mitoxantrone, etoposide, dactinomycin), RNA transcription (i.e. dinaciclib, THZ2, alvocidib, fludarabine), protein signalling (i.e. AMG-232, UCN-01, pictilisib, triciribine) or cytoskeleton (i.e. idasanutiin , indibulin, vinorelbine), and, therefore, damaged DNA, RNA and proteins (Fig. 5d). Thus, these agents induced p53-dependent Bcl-xL-mediated apoptosis, i.e. Bcl-xL was essential for induction of apoptosis in non-malignant cells treated with RNA, DNA or protein-damaging agents.

Exploiting p53-dependent Bcl-xL-mediated apoptosis for identification of chemical agents, which damage cellular DNA, RNA or proteins

Next, we tested monomeric bisbenzimidazole-pyrrole MB2Py(Ac), dimeric benzimidazole-pyrroles DB2Py(4) and DB2Py(5), as well as dimeric bisbenzimidazoles DBA(3), DBA(5), and DBA(7) on A-1155463-sensitized and non-sensitized RPE cells. These 6 molecules were developed to bind minor groove of DNA (Ivanov, Susova et al., 2013, Koval, Arutyunyan et al., 2018). MB2Py(Ac), DB2Py(4) and DB2Py(5), but not DBA(3), DBA(5), and DBA(7), primed A-1155463-sensitized cells for apoptosis (Fig. 6a). The synergy scores calculated using 3 highest doses of MB2Py(Ac), DB2Py(4) and DB2Py(5) were 6 , 5 and 4, respectively, whereas for DBA(3), DBA(5), and DBA(7) they were -11, -16, and -14, respectively.

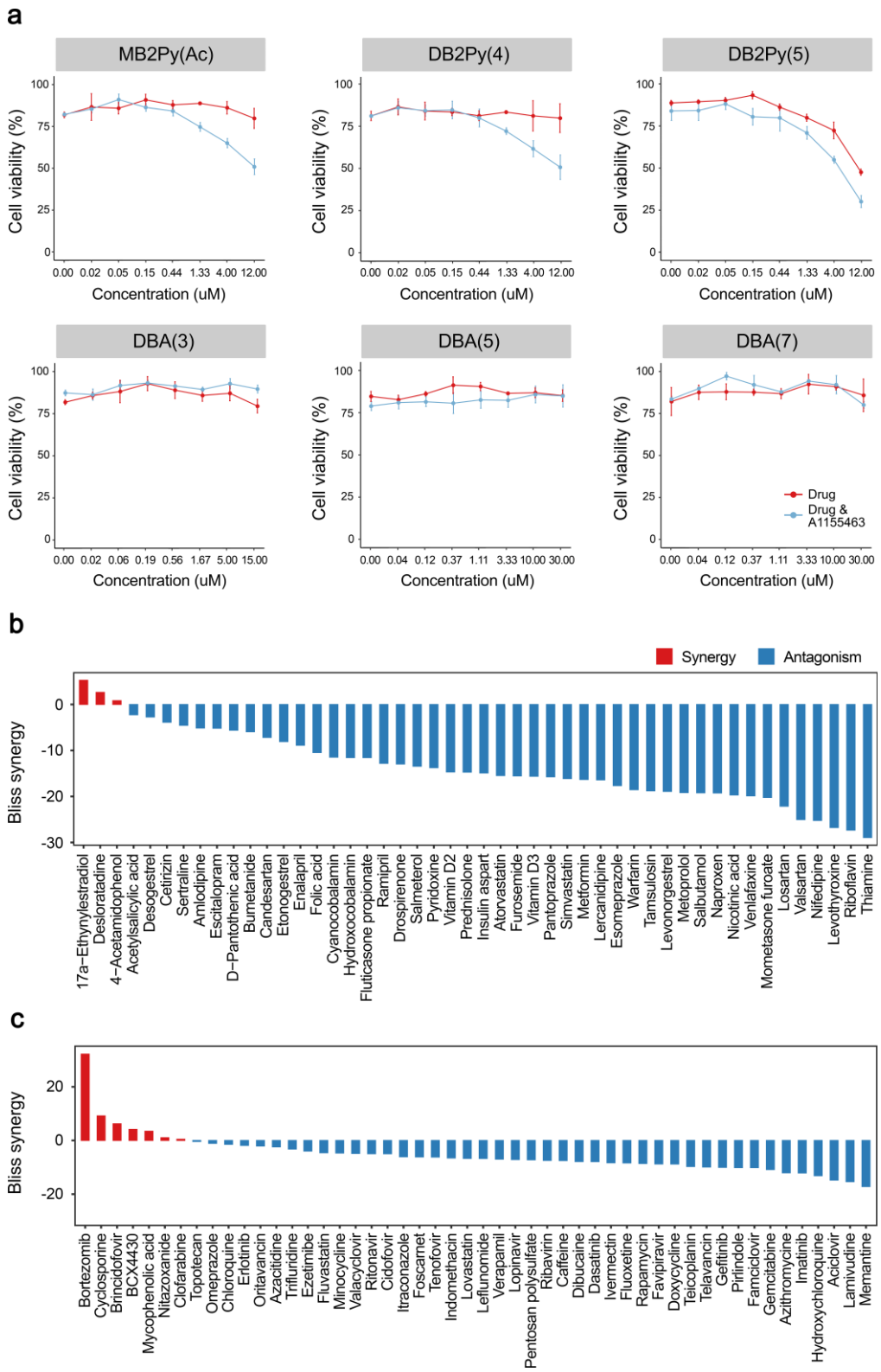

Figure 6. Exploiting p53-dependent Bcl-xL-mediated apoptosis for identification of chemical agents, which damage cellular DNA, RNA or proteins. (a) Effect of different concentrations of dimeric bisbenzimidazoles DBA(3), DBA(5) and DBA(7), monomeric bisbenzimidazole-pyrrole MB2Py(Ac) and dimeric benzimidazole-pyrroles DB2Py(4) and DB2Py(5) on viability of A-1155463-sensitized (1

μM) and non-sensitized (0.1% DMSO) RPE cells. Mean ± SD, n = 3. (b) Bliss synergy scores for A-1155463 and 48 commonly dispensed drugs. A-1155463-sensitized (1 μM) and non-sensitized (0.1% DMSO) RPE cells were treated with 0, 0.1, 0.4, 1.2, 3.7, 11.1, 33.3, and 100 μM of drugs. After 24 h cell viability was measured by the CTG assay (n=3). (c) Bliss synergy scores for A-1155463 and 50 safe-in-man broad-spectrum antiviral agents. A-1155463-sensitized (1 μM) and non-sensitized (0.1% DMSO) RPE cells were treated with 0, 0.04, 0.12, 0.37, 1.11, 3.33, 10, and 30 μM of antiviral agents. After 24 h cell viability was measured by the CTG assay (n=3).

Given that DB2Py(4) and DB2Py(5) differed from DBA(n) molecules by the pyrrole fragment and the N-methylpiperazine end group (instead of dimethylaminopropylamide; Fig. S3), these differences appeared to be essential for initiation of apoptosis in A-1155463-sensitized RPE cells. Moreover, dimerization of B2Py(n) was not essential for Bcl-xL-mediated apoptosis, since both MB2Py(Ac) and DB2Py(n) had similar synergy scores. Most probably, MB2Py(Ac) bound minor groove of cellular DNA and altered pol II transcription, which led to accumulation of aberrant RNA transcripts, that triggered apoptosis in A-1155463-sensitized RPE cells. Thus, the MB2Py(Ac), DB2Py(4) and DB2Py(5) possessed DNA-binding activity that could interfere with general transcription.

We further exploited Bcl-xL-mediated apoptosis for identification of chemical agents that damaged cellular DNA, RNA or proteins. We tested 48 drugs commonly dispensed in Norway and 50 safe-in-man broad-spectrum antiviral agents. We found that 17α-ethynylestradiol, bortezomib, cyclosporin and brincidofovir primed A-1155463-sensitized RPE cells for apoptosis (Bliss synergy score >6). These results indicated that 17α-ethynylestradiol, cyclosporin and brincidofovir could damage cellular DNA, RNA or proteins and subsequently could induce apoptosis (Fig. 6b,c). Moreover, we confirmed that bortezomib impaired protein degradation, which could be associated with accumulation of damaged proteins, which triggered Bcl-xL-mediated apoptosis (Kim, Song et al., 2014).

Exploiting p53-dependent Bcl-xL-mediated apoptosis for identification of physical factors that damage cellular DNA, RNA or proteins

We next exposed A-1155463-sensitized and non-sensitized RPE cells to UVB and UVC radiation, which similarly to the 4NQO treatment, induced lesions in DNA (Walker & Sridhar, 1975). After 24 h the cell viability was measured using the CTG assay. We observed that already 8 sec of exposure UV killed A-1155463-sensitized but not non-sensitized RPE cells (Bliss synergy scores: 31.2 and 23.8, respectively; Fig. 7). This indicated that UVB and UVC triggered Bcl-xL-mediated apoptosis.

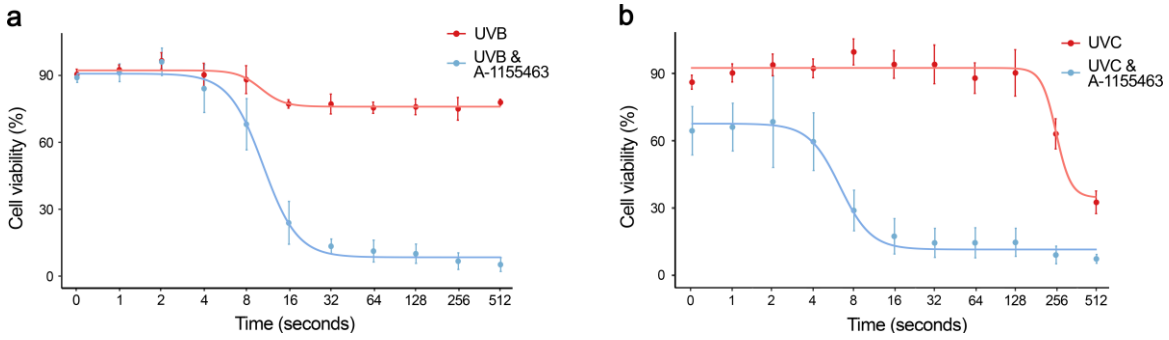

Figure 7. UV radiation kills A-1155463-sensitized, but not non-sensitized RPE cells. RPE cells were exposed to UVB (a) and UVC (b) radiation for the indicated times and covered with medium containing 1 μM A-1155463 or 0.1% DMSO. After 24 h, viability of cells was measured using the CTG assay. Mean ± SD, n = 3.

DISCUSSION

Here we developed a method to identify physical, chemical and biological factors which trigger Bcl-xL-mediated apoptosis. We used the method to show that anticancer agents targeting DNA replication (i.e. amsacrine, SN38, cisplatin, mitoxantrone, etoposide, dactinomycin), RNA transcription (i.e. 4NQO, dinaciclib, THZ2, alvocidib, fludarabine), protein signalling (i.e. AMG-232, UCN-01, pictilisib, triciribine) or cytoskeleton (i.e. idasanutib, indibulin, vinoirelbine) killed cells sensitized with Bcl-xL-, but not Bcl-2- or Mcl-1-specific inhibitors. Moreover, we found that DNA binding probes MB2Py(Ac), DB2Py(4) and DB2Py(5), birth-control drug 17α-ethynylestradiol, immunosuppressant cyclosporin, antiviral agent brincidofovir, as well as UVB and UVC radiation killed A-1155463-sencitized cells.

In addition, we demonstrated that DNA-damaging agent 4NQO killed human non-malignant and malignant cells, as well as small roundworm C. elegans, which were sensitized with A-1155463. The cell death was dependent on the concentration of both agents. The synergistic effect of 4NQO-A-1155463 combination was p53 dependent and was associated with the release of Bad and Bax from Bcl-xL. Our results suggest that intracellular receptors sensed damaged DNA, transmitted this information via p53 to anti-apoptotic Bcl-xL, which released pro-apoptotic Bax and Bad to trigger cell death. Thus, Bcl-xL protein could serve as ‘safety fuse’, which mediated apoptosis, when concentration of damaged cellular factors reached critical levels (Fig. 8).

We showed recently that non-malignant cells infected with viruses or transfected with viral RNA or plasmid DNA were also sensitive to Bcl-xL-specific inhibitor A-1155463 (Bulanova, Ianevski et al., 2017, Kakkola et al., 2013, Shim et al., 2017). This indicate that invasive RNA or DNA could also trigger Bcl-xL-mediated apoptosis (Fig. 8).

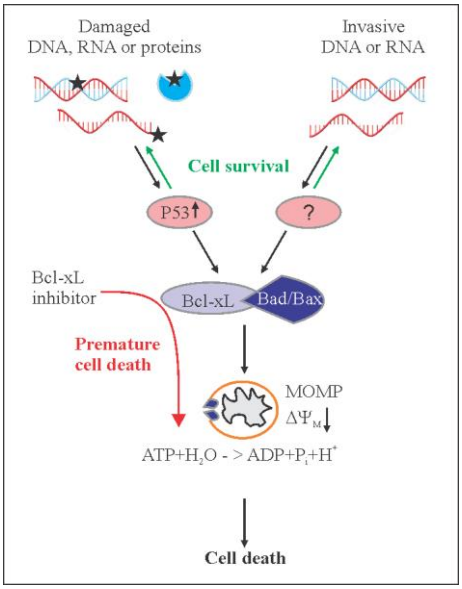

Figure 8. Schematic diagram showing how apoptosis could be initiated in response to chemical and physical stimuli or viruses, and how Bcl-xL-specific inhibitors could facilitate this process. Damage response (DR) factors and pattern recognition receptors (PRRs) recognize damaged molecules and invasive DNA or RNA, respectively. These proteins transduce signals to Bcl-xL via p53 or other protein(s). Pro-apoptotic Bax and Bad are released from anti-apoptotic Bcl-xL. When concentration of damaged or invasive molecules reach critical level, released Bax and Bad trigger mitochondrial outer membrane permeabilization (MoMP), which lead to inhibition of ATP synthesis, irreversible release of intermembrane space proteins, and subsequent caspase activation. This results in cell death. Alternatively, DR proteins and PRRs could mediate repair or degradation of damaged or invasive molecules, respectively, which would leave cells alive. Bcl-xL-specific inhibitors facilitate death of cells and, thus, impair repair or degradation of damaged or invasive factors.

Importantly, locally induced Bcl-xL mediated apoptosis could have a clinical potential for treatment of tumors. For example, skin cancers could be treated with systemic Bcl-xL-specific inhibitor and topical UV radiation, oncolytic virus infection or combinational anticancer medication. Recent studies support this idea by showing, for example, that combination of radiotherapy with pan-Bcl-2 inhibitors ABT-737 and ABT-263 killed breast and small cell lung cancer cells *in vitro* (Table S2) (Li, Wang et al., 2019, Wu, Schiff et al., 2014). Moreover, ABT-737 sensitized chronic lymphocytic leukaemia cells to reovirus and vesicular stomatitis oncolysis (Samuel, Beljanski et al., 2013). Further *in vivo* studies are needed to exploit locally-induced Bcl-xL mediated apoptosis for cancer treatment.

In conclusion, we developed a method for identification of physical, chemical and biological factors that induced Bcl-xL-mediated apoptosis. This method could provide novel opportunities for discovery of therapeutic and adverse effects of anticancer medications. It also could be used to identify conditions, which would prevent other non-communicable and communicable diseases as well as aging, given that cells with high concentration of damaged DNA, RNA or proteins or with invasive DNA and RNA molecules would be eliminated from an organism receiving a Bcl-xL-specific inhibitor.

MATERIALS AND METHODS

Bcl2iCombi database

We reviewed developmental status of Bcl-2 inhibitors and their combinations with other anticancer therapeutics. We summarized the information in freely accessible database (bcl2icombi.info). The drug annotations were obtained from PubChem, DrugBank, DrugCentral, PubMed and clinicaltrials.gov databases (Table S1) (Kim, Chen et al., 2019, Ursu, Holmes et al., 2019, Wishart, Feunang et al., 2018). The database summarizes activities and developmental stages of the drug combinations. The database allows interactive exploration of drug-drug and drug-target interactions. A feedback form is available on the website. The database will be updated upon request or as soon as a new drug combination is reported.

Compounds

ABT-199 (CAS: 1257044-40-8), A-1331852 (CAS: 1430844-80-6), A-1155463 (CAS: 1235034-55-5), and S63845 (CAS: 1799633-27-4) were purchased from Selleck Chemicals (Houston, TX, USA). 4NQO (CAS: 56-57-5) was from Merck Life Science (Espoo, Finland). Dimeric bisbenzimidazoles DBA(3), DBA(5) and DBA(7) were synthesized as described previously (Koval et al., 2018). Monomeric MB2Py(Ac) and dimeric DB2Py(4) and DB2Py(5) benzimidazole-pyrroles were also described previously (Ivanov et al., 2013). A library of 527 approved and emerging investigational oncology drugs were from the collection of the Institute of Molecular Medicine Finland, FIMM (www.fimm.fi/en/services/technology-centre/htb/equipment-and-libraries/chemical-libraries). A library of 48 drugs commonly dispensed in Norway was assembled based on Norwegian Prescription Database (www.norpd.no). Table S1 lists these compounds, their suppliers and catalogue numbers. A library of 50 safe-in-man broad-spectrum antivirals was published previously (Ianevski, Zusinaite et al., 2018). To obtain 10 mM stock solutions, compounds were dissolved in dimethyl sulfoxide (DMSO, Sigma-Aldrich, Steinheim, Germany) or milli-Q water. The solutions were stored at −80 °C until use.

Cells

Human telomerase reverse transcriptase-immortalized retinal pigment epithelial (RPE, ATCC) cells were grown in DMEM-F12 medium supplemented with 100 U/ml penicillin/streptomycin (Pen/Strep), 2 mM L-glutamine, 10% FBS, and 0.25% sodium bicarbonate (Sigma-Aldrich, St. Louis, USA) or RPMI medium supplied with 10% FBS and Pen-Strep. Human colon cancer cell lines HCT116 *TP53*$^{+/+}$ and HCT116 *TP53*$^{-/-}$ were grown in McCoy's 5A Medium (Sigma, M9309) supplemented with 10% FBS and Pen/Strep. The cell lines were maintained at 37°C with 5% CO2.

C. elegans maintenance, lifespan and toxicity assays

Standard *C. elegans* strain maintenance procedures were followed in all experiments (Brenner, 1974, Fang, Hou et al., 2019, Fang, Kassahun et al., 2016, Fang, Scheibye-Knudsen et al., 2014). Nematode rearing temperature was kept at 20 °C, unless noted otherwise. N2: wild type Bristol isolate was from Caenorhabditis Genetics Center (CGC).

For lifespan experiments, gravid adult worms were placed on NGM plates containing either A-1155463 (10 µM), 4NQO (10 µM), combination A-1155463 (10 µM) + 4NQO (10 µM) or vehicle control and seeded with OP50 to lay eggs. Progeny were grown at 20°C through the L4 larval stage and then transferred to fresh plates in groups of 30-35 worms per plate for a total of 100 individuals per experimental condition. Animals were transferred to fresh plates every 2–4 days thereafter and examined every other day for touch-provoked movement and pharyngeal pumping, until death. Worms that died owing to internally hatched eggs, an extruded gonad or desiccation due to crawling on the edge of the plates were censored and incorporated as such into the data set. Survival curves were created using the product-limit method of Kaplan and Meier. The log-rank (Mantel–Cox) test was used for statistical analysis.

A series of toxicity *e*xperiments, including fecundity, egg hatching, larval development, were conducted using N2 Bristol isolate *C. elegans*, which were cultivated as previously described (Brenner, 1974) and maintained at 20°C. Briefly, for the toxicity assay animals were initially synchronised by bleaching gravid adults (adult day 1-4) to extract the eggs. Eggs were placed on nematode growth medium (NGM) plates seeded with *Escherichia coli* (OP50). L4 larvae were subsequently transferred onto fresh OP50-seeded NGM plates and allowed to grow to adulthood. Ten adult day 1 worms (n = 30-50/experimental condition) were transferred onto assay NGM plates with OP50 containing either A-1155463 (1, 10, 100 µM), 4NQO (1, 10, 100 µM), combination A-1155463 (10 µM) plus 4NQO (2, 10, 20 µM) or vehicle control. Animals laid eggs for three hours. Subsequently, adults were removed from the plate and the frequency of eggs laid was quantified as a measure of reproduction and egg-laying capacity of worms. The following day the frequency of unhatched eggs and L1 larvae were counted in order to evaluate the efficiency of egg hatching. Subsequently, 36 h later, development to L4 larvae was assessed, as a measure of larval growth. Finally, growth of L4 larvae to adulthood was quantified after 16 h.

The toxicity assay was conducted at 20°C on 10 ml NGM plates seeded with 100 µl OP50 from an overnight culture. Drug compounds and vehicle solvents were dissolved in a total volume of 200 µl, sufficient to cover the entire surface of the plate, and were dried at room temperature for 1-2 h prior to the transfer of worms. Each chemical concentration was tested three-five times. Statistical analysis was conducted using One-Way ANOVA followed by Tukey's multiple comparison test.

Real-time impedance assay

RPE cells were grown at 37°C in 16-well E-Plates to 90% confluency. The plates were supplied with golden electrodes at the bottom of the wells and a weak electrical current was constantly applied to the cell medium. The changes in the cell adherence indexes (CI) were monitored by the xCELLigence real-time drug cytotoxicity system (ACEA Biosciences, San Diego, USA) as described previously

(Solly, Wang et al., 2004). When cells reached 90% confluency, 1 µM 4NQO, 1 µM A-1155463 or their combination were added. Control cells were treated with 0.01% of DMSO. CI were normalized and monitored for another 24 hours.

Cell viability assay

Approximately, $4x10^4$ RPE or HCT116 cells per well of 96-well plate were treated with A-1155463, 4NQO or both compounds. Control cells were treated with 0.01% of DMSO. After 24 or 48 h, respectively, the viability of cells was measured using the Cell Titer Glo assay (CTG, Promega). Luminescence was measured using PerkinElmer Victor X3 or Synergy Mx plate readers.

Cell toxicity assay

Approximately, $4x10^4$ HCT116 cells per well of 96-well plate were treated with 1 µM 4NQO, 1 µM A-1155463 or their combination. Control cells were treated with 0.01% of DMSO. After 24 h, the death of cells was detected using the Cell Toxicity Assay (CTxG, Promega). Fluorescence was measured using PerkinElmer Victor X3 Reader.

Early apoptosis assay

Approximately, $4x10^4$ RPE, HCT116 *TP53*$^{+/+}$ or *TP53*$^{-/-}$ cells per well of 96-well plate were treated with 1 µM 4NQO, 1 µM A-1155463 or their combination. Control cells were treated with 0.01% of DMSO. Activation of apoptosis was assessed using RealTime-Glo Annexin V Apoptosis and Necrosis Assay (Promega). Luminescence was measured using PerkinElmer Victor X3 Reader.

Apoptosis and phospho-kinase arrays

Approximately, $1x10^6$ RPE cells per well of 6-well plate were treated with 1 µM 4NQO, 1 µM A-1155463 or their combination. Control cells were treated with 0.01% of DMSO. After 2 h, relative levels of apoptosis-related proteins and protein kinase phosphorylation were determined using proteome profiler human apoptosis and human phospho-kinase array kits, respectively, as described in the manuals (R&D Systems, Minneapolis, MN, USA). Membranes were scanned using Odyssey Li-Cor system.

Metabolic labelling of cellular RNA and proteins

Approximately, $1x10^5$ RPE cells per well of 12-well plate were treated with 1 µM 4NQO, 1 µM A-1155463 or their combination dissolved in 500 µl cell growth medium. Control cells were treated with 0.01% of DMSO. The medium was supplemented with 3 µl of [alpha-P32]UTP (9,25 MBq, 250 µCi in 25 µl). Cells were incubated for 2 h at 37 °C. Cells were washed twice with PBS. Total RNA was isolated using RNeasy Plus extraction kit (Qiagen, Hilden, Germany). RNA was separated on 1%

agarose gel. Gel was dried. Total RNA was detected using Ethidium Bromide. ^{32}P-labeled RNA was monitored using radioautography and visualised using Typhoon 9400 scanner (GE Healthcare).

In a parallel experiment, the compounds or DMSO were added to 500 µl cysteine- and methionine-free DMEM medium (Sigma-Aldrich, Germany) containing 10% BSA and 3 µl [^{35}S] EasyTag Express protein labelling mix (7 mCi, 259 MBq, 1175 Ci/mmol in 632 ml; Perkin Elmer, Espoo, Finland). After 2 h of incubation at 37 °C cells were washed twice with PBS, lysed in 2 × SDS-loading buffer and sonicated. Lysates were loaded and proteins were separated on a 10% SDS-polyacrylamide gel. ^{35}S-labelled proteins were monitored using radioautography and visualised using a Typhoon 9400 scanner (GE Healthcare).

UV radiation assay

RPE cells were exposed to UVC (λ = 254 nm) or to UVB (λ = 302 nm) using Hoefer UVC 500 Ultraviolet Crosslinker (20 J/cm2) or VM25/30/GX trans-illuminator as UV sources, respectively. 1 µM A-1155463 or 0.1% DMSO were added to the cell medium. After 24 h viability of cells was measured using CTG assay (Promega, Madison, USA). The luminescence was read with a PHERAstar FS plate reader (BMG Labtech, Ortenberg, Germany).

Synergy calculations

RPE cells were treated with different concentrations of a Bcl-2 inhibitor and another drug. After 24 h cell viability was measured using CTG assay. To test whether the drug combinations act synergistically, the observed responses were compared with expected combination responses. The expected responses were calculated based on Bliss reference model using SynergyFinder web-application (Ianevski, He et al., 2017). For in vitro combinatorial experiments where the whole dose-response matrix was measured, a normalized Bliss reference model, i.e. Zero Interaction Potency (ZIP) model was utilized.

Immuno-precipitation and immuno-blotting

RPE cells remained untreated or were treated with 1 µM A-1155463, 1 µM 4NQO or their combination for 2 h. Cells were lysed in buffer containing 20 mM Tris-HCl, 0.5% NP-40, 150 mM NaCl, 1.5 mM MgCl2, 10 mM KCl, 10% Glycerol, 0.5 mM EDTA, pH 7.9 and protease inhibitor cocktail (Sigma). Bcl-xL-associated factors were immuno-precipitated using rabbit anti-Bcl-xL antibody (Cell Signaling Technology) immobilized on the magnetic Protein G Dynabeads (Thermo Fisher Scientific). Normal rabbit IgG (Santa Cruz Biotechnology, sc-2025) was used to control immunoprecipitation with an equal volume of cell lysate. The immobilized protein complexes together with the appropriate whole-cell extract inputs were subjected for SDS-PAGE followed by immunoblotting.

Proteins were transferred to nitrocellulose membrane (Sartorius). The membranes were blocked with 10% BSA (Santa Cruz Biotechnology) in TBS. Primary antibodies (rabbit anti-Bax, 1:1000; N-20, sc-493, rabbit anti-BAD, 1 : 1000; clone D24A9; Santa Cruz Biotechnology, mouse anti-p53, 1 : 1000;

Santa Cruz Biotechnology, sc-126 and mouse anti-GAPDH, 1 : 1000; Santa Cruz Biotechnology, sc-32233; Bcl-xL antibody, 1 : 1000, Cell Signalling Technology) were diluted in TBS and added to the membranes. After overnight incubation at 4 °C, membranes were washed three times with TBS buffer containing 0.03% Tween 20 (Tween/TBS). Secondary antibodies conjugated to HRP (Santa Cruz Biotechnology, anti-mouse: m-IgGκ BP-HRP, sc-516102; anti-rabbit mouse anti-rabbit IgG-HRP, sc-2357) were added. Chemiluminescence was detected using the Western Lightning Chemiluminescence Reagent (Perkin Elmer) by ChemiDoc Imaging System (BioRad).

HCT116 *TP53*$^{+/+}$ and *TP53*$^{-/-}$ cells remained untreated or were treated with 1 μM A-1155463, 1 μM 4NQO or both compounds. After 16 h, cells were lysed, and proteins were separated using 4-20% gradient SDS-PAGE. The proteins were transferred to a Hybond-LFP PVDF membrane. The membranes were blocked using 5% milk in Tris-buffered saline (TBS). p53 and GAPDH were detected using mouse anti-p53 and mouse anti-GAPDH antibodies as described above.

Confocal microscopy

RPE cells were treated with 1 μM A-1155463, 1 μM 4NQO or both compounds. Control cells were treated with 0,1% DMSO. After 1 and 2 h cells were fixed using 3.3% formaldehyde in 10% FBS and PBS, pH 7.4. Cells were permeabilized using 10% FBS and 0.1% Triton X-100 in PBS. Bad, Bax (2 different antibodies), Bcl-xL, p53 and Tom40 were detected using rabbit anti-Bcl-xL (1 : 250; clone 54H6; Cell Signalling Technology), mouse anti-Bax (1:250; 2D2, sc-20067), rabbit anti-Bax (1:250; N-20, sc-493), rabbit anti-BAD (1:250; clone D24A9; Santa Cruz Biotechnology), mouse anti-p53 (1 : 250; Santa Cruz Biotechnology) and anti-Tom40 (1:250; Santa Cruz Biotechnology, sc-11414) antibodies were used. Secondary goat anti-mouse IgG (H+L) Alexa Fluor® 488 and 568 (Thermo Scientific), goat anti-rabbit IgG (H+L) Alexa Fluor® 488 and 568 (Thermo Scientific) antibodies were used. ProLong™ Gold Antifade Mountant (Invitrogen) with DAPI was used for mounting of cells. Cells were imaged using Zeiss LSM710 confocal microscope.

SUPPLEMENTARY DATA

Supplementary Data are available online.

ACKNOWLEDGEMENT

We thank Hege Ramstad, Jelena Kiprovskaja, Eva Zusinaite, Alun Parson and Laivi Karu for assistance. We also thank the DDCB core facility supported by the University of Helsinki and Biocenter Finland.

FUNDING

This work was supported by NTNU-Digital micro-sabbatical stipend, the European Regional Development Fund the Mobilitas Pluss Project [70441712/630110, MOBTT39 to D.E.K.], HELSE SøR-ØST, the Research Council of Norway and Rosa Sløyfe, Norwegian Breast Cancer Society

[2017056, 262175, 2020001, 207819 to E.F.F.], and Russian Foundation for Basic Research [19-04-00206 to A.L.Z.]. Funding for open access charge: University of Tartu.

CONFLICT OF INTEREST

E.F.F. has CRADA arrangements with ChromaDex and is a consultant to Aladdin Healthcare Technologies and the Vancouver Dementia Prevention Centre. All others declare no competing interests.

REFERENCES

Adams CM, Clark-Garvey S, Porcu P, Eischen CM (2018) Targeting the Bcl-2 Family in B Cell Lymphoma. *Front Oncol* 8: 636

Brenner S (1974) The genetics of Caenorhabditis elegans. *Genetics* 77: 71-94

Bulanova D, Ianevski A, Bugai A, Akimov Y, Kuivanen S, Paavilainen H, Kakkola L, Nandania J, Turunen L, Ohman T, Ala-Hongisto H, Pesonen HM, Kuisma MS, Honkimaa A, Walton EL, Oksenych V, Lorey MB, Guschin D, Shim J, Kim J et al. (2017) Antiviral Properties of Chemical Inhibitors of Cellular Anti-Apoptotic Bcl-2 Proteins. *Viruses* 9

Casara P, Davidson J, Claperon A, Le Toumelin-Braizat G, Vogler M, Bruno A, Chanrion M, Lysiak-Auvity G, Le Diguarher T, Starck JB, Chen I, Whitehead N, Graham C, Matassova N, Dokurno P, Pedder C, Wang Y, Qiu S, Girard AM, Schneider E et al. (2018) S55746 is a novel orally active BCL-2 selective and potent inhibitor that impairs hematological tumor growth. *Oncotarget* 9: 20075-20088

Chen J, Jin S, Abraham V, Huang X, Liu B, Mitten MJ, Nimmer P, Lin X, Smith M, Shen Y, Shoemaker AR, Tahir SK, Zhang H, Ackler SL, Rosenberg SH, Maecker H, Sampath D, Leverson JD, Tse C, Elmore SW (2011) The Bcl-2/Bcl-X(L)/Bcl-w inhibitor, navitoclax, enhances the activity of chemotherapeutic agents in vitro and in vivo. *Mol Cancer Ther* 10: 2340-9

Denisova OV, Kakkola L, Feng L, Stenman J, Nagaraj A, Lampe J, Yadav B, Aittokallio T, Kaukinen P, Ahola T, Kuivanen S, Vapalahti O, Kantele A, Tynell J, Julkunen I, Kallio-Kokko H, Paavilainen H, Hukkanen V, Elliott RM, De Brabander JK et al. (2012) Obatoclax, saliphenylhalamide, and gemcitabine inhibit influenza a virus infection. *J Biol Chem* 287: 35324-32

Elmore S (2007) Apoptosis: a review of programmed cell death. *Toxicol Pathol* 35: 495-516

Fang EF, Hou Y, Palikaras K, Adriaanse BA, Kerr JS, Yang B, Lautrup S, Hasan-Olive MM, Caponio D, Dan X, Rocktaschel P, Croteau DL, Akbari M, Greig NH, Fladby T, Nilsen H, Cader MZ, Mattson MP, Tavernarakis N, Bohr VA (2019) Mitophagy inhibits amyloid-beta and tau pathology and reverses cognitive deficits in models of Alzheimer's disease. *Nat Neurosci* 22: 401-412

Fang EF, Kassahun H, Croteau DL, Scheibye-Knudsen M, Marosi K, Lu H, Shamanna RA, Kalyanasundaram S, Bollineni RC, Wilson MA, Iser WB, Wollman BN, Morevati M, Li J, Kerr JS, Lu Q, Waltz TB, Tian J, Sinclair DA, Mattson MP et al. (2016) NAD+ Replenishment Improves Lifespan and Healthspan in Ataxia Telangiectasia Models via Mitophagy and DNA Repair. *Cell Metab* 24: 566-581

Fang EF, Scheibye-Knudsen M, Brace LE, Kassahun H, SenGupta T, Nilsen H, Mitchell JR, Croteau DL, Bohr VA (2014) Defective mitophagy in XPA via PARP-1 hyperactivation and NAD(+)/SIRT1 reduction. *Cell* 157: 882-896

Fernandez AF, Sebti S, Wei Y, Zou Z, Shi M, McMillan KL, He C, Ting T, Liu Y, Chiang WC, Marciano DK, Schiattarella GG, Bhagat G, Moe OW, Hu MC, Levine B (2018) Disruption of the beclin 1-BCL2 autophagy regulatory complex promotes longevity in mice. *Nature* 558: 136-140

Haikala HM, Anttila JM, Marques E, Raatikainen T, Ilander M, Hakanen H, Ala-Hongisto H, Savelius M, Balboa D, Von Eyss B, Eskelinen V, Munne P, Nieminen AI, Otonkoski T, Schuler J, Laajala TD, Aittokallio T, Sihto H, Mattson J, Heikkila P et al. (2019) Pharmacological reactivation of MYC-dependent apoptosis induces susceptibility to anti-PD-1 immunotherapy. *Nat Commun* 10: 620

Ianevski A, He L, Aittokallio T, Tang J (2017) SynergyFinder: a web application for analyzing drug combination dose-response matrix data. *Bioinformatics* 33: 2413-2415

Ianevski A, Zusinaite E, Kuivanen S, Strand M, Lysvand H, Teppor M, Kakkola L, Paavilainen H, Laajala M, Kallio-Kokko H, Valkonen M, Kantele A, Telling K, Lutsar I, Letjuka P, Metelitsa N, Oksenych V, Bjoras M, Nordbo SA, Dumpis U et al. (2018) Novel activities of safe-in-human broad-spectrum antiviral agents. *Antiviral Res* 154: 174-182

Ivanov AA, Susova OY, Salyanov VI, Kirsanov KI, Zhuze AL (2013) A new series of biologically active DNA minor groove binders based on bisbenzimidazole and benzimidazole-pyrrole motives. *Journal of Biomolecular Structure and Dynamics* 31

Jeong JH, Oh JM, Jeong SY, Lee SW, Lee J, Ahn BC (2019) Combination Treatment with the BRAF(V600E) Inhibitor Vemurafenib and the BH3 Mimetic Navitoclax for BRAF-Mutant Thyroid Carcinoma. *Thyroid* 29: 540-548

Kakkola L, Denisova OV, Tynell J, Viiliainen J, Ysenbaert T, Matos RC, Nagaraj A, Ohman T, Kuivanen S, Paavilainen H, Feng L, Yadav B, Julkunen I, Vapalahti O, Hukkanen V, Stenman J, Aittokallio T, Verschuren EW, Ojala PM, Nyman T et al. (2013) Anticancer compound ABT-263 accelerates apoptosis in virus-infected cells and imbalances cytokine production and lowers survival rates of infected mice. *Cell Death Dis* 4: e742

Kale J, Osterlund EJ, Andrews DW (2018) BCL-2 family proteins: changing partners in the dance towards death. *Cell Death Differ* 25: 65-80

Kim S, Chen J, Cheng T, Gindulyte A, He J, He S, Li Q, Shoemaker BA, Thiessen PA, Yu B, Zaslavsky L, Zhang J, Bolton EE (2019) PubChem 2019 update: improved access to chemical data. *Nucleic Acids Res* 47: D1102-D1109

Kim SY, Song X, Zhang L, Bartlett DL, Lee YJ (2014) Role of Bcl-xL/Beclin-1 in interplay between apoptosis and autophagy in oxaliplatin and bortezomib-induced cell death. *Biochem Pharmacol* 88: 178-88

King AC, Peterson TJ, Horvat TZ, Rodriguez M, Tang LA (2017) Venetoclax: A First-in-Class Oral BCL-2 Inhibitor for the Management of Lymphoid Malignancies. *Ann Pharmacother* 51: 410-416

Korycka-Wolowiec A, Wolowiec D, Kubiak-Mlonka A, Robak T (2019) Venetoclax in the treatment of chronic lymphocytic leukemia. *Expert Opin Drug Metab Toxicol* 15: 353-366

Koval VS, Arutyunyan AF, Salyanov VL, Klimova RR, Kushch AA, Rybalkina EY, Susova OY, Zhuze AL (2018) DNA sequence-specific ligands. XVII. Synthesis, spectral properties, virological and biochemical studies of fluorescent dimeric bisbenzimidazoles DBA(n). *Bioorg Med Chem* 26: 2302-2309

Kuivanen S, Bespalov MM, Nandania J, Ianevski A, Velagapudi V, De Brabander JK, Kainov DE, Vapalahti O (2017) Obatoclax, saliphenylhalamide and gemcitabine inhibit Zika virus infection in vitro and differentially affect cellular signaling, transcription and metabolism. *Antiviral Res* 139: 117-128

Lai PB, Chi TY, Chen GG (2007) Different levels of p53 induced either apoptosis or cell cycle arrest in a doxycycline-regulated hepatocellular carcinoma cell line in vitro. *Apoptosis* 12: 387-93

Li H, Wang H, Deng K, Han W, Hong B, Lin W (2019) The ratio of Bcl-2/Bim as a predictor of cisplatin response provides a rational combination of ABT-263 with cisplatin or radiation in small cell lung cancer. *Cancer Biomark* 24: 51-59

Samuel S, Beljanski V, Van Grevenynghe J, Richards S, Ben Yebdri F, He Z, Nichols C, Belgnaoui SM, Steel C, Goulet ML, Shamy A, Brown D, Abesada G, Haddad EK, Hiscott J (2013) BCL-2 inhibitors sensitize therapy-resistant chronic lymphocytic leukemia cells to VSV oncolysis. *Mol Ther* 21: 1413-23

Shamas-Din A, Kale J, Leber B, Andrews DW (2013) Mechanisms of action of Bcl-2 family proteins. *Cold Spring Harb Perspect Biol* 5: a008714

Shen Q, Li J, Mai J, Zhang Z, Fisher A, Wu X, Li Z, Ramirez MR, Chen S, Shen H (2018) Sensitizing non-small cell lung cancer to BCL-xL-targeted apoptosis. *Cell Death Dis* 9: 986

Shim JM, Kim J, Tenson T, Min JY, Kainov DE (2017) Influenza Virus Infection, Interferon Response, Viral Counter-Response, and Apoptosis. *Viruses* 9

Solly K, Wang X, Xu X, Strulovici B, Zheng W (2004) Application of real-time cell electronic sensing (RT-CES) technology to cell-based assays. *Assay Drug Dev Technol* 2: 363-72

Timucin AC, Basaga H, Kutuk O (2019) Selective targeting of antiapoptotic BCL-2 proteins in cancer. *Med Res Rev* 39: 146-175

Ursu O, Holmes J, Bologa CG, Yang JJ, Mathias SL, Stathias V, Nguyen DT, Schurer S, Oprea T (2019) DrugCentral 2018: an update. *Nucleic Acids Res* 47: D963-D970

Walker IG, Sridhar R (1975) Alkali-labile lesions in DNA from cells treated with methylating agents, 4-nitroquinoline-N-oxide, or ultraviolet light. *Basic Life Sci* 5A: 29-30

Wishart DS, Feunang YD, Guo AC, Lo EJ, Marcu A, Grant JR, Sajed T, Johnson D, Li C, Sayeeda Z, Assempour N, Iynkkaran I, Liu Y, Maciejewski A, Gale N, Wilson A, Chin L, Cummings R, Le D, Pon A et al. (2018) DrugBank 5.0: a major update to the DrugBank database for 2018. *Nucleic Acids Res* 46: D1074-D1082

Wong RS (2011) Apoptosis in cancer: from pathogenesis to treatment. *J Exp Clin Cancer Res* 30: 87

Wu H, Schiff DS, Lin Y, Neboori HJ, Goyal S, Feng Z, Haffty BG (2014) Ionizing radiation sensitizes breast cancer cells to Bcl-2 inhibitor, ABT-737, through regulating Mcl-1. *Radiat Res* 182: 618-25